Aggregation Latency-Energy Tradeoff in Wireless Sensor Networks with Successive Interference Cancellation

Hongxing Li, *Member*, *IEEE*, Chuan Wu, *Member*, *IEEE*, Dongxiao Yu, Qiang-Sheng Hua, *Member*, *IEEE*, and Francis C.M. Lau, *Senior Member*, *IEEE*

Abstract—Minimizing latency and energy consumption is the prime objective of the design of data aggregation in battery-powered wireless networks. A tradeoff exists between the aggregation latency and the energy consumption, which has been widely studied under the protocol interference model. There has been, however, no investigation of the tradeoff under the physical interference model that is known to capture more accurately the characteristics of wireless interferences. When coupled with the technique of *successive interference cancellation*, by which a receiver may recover signals from multiple simultaneous senders, the model can lead to much reduced latency but increased energy usage. In this paper, we investigate the latency-energy tradeoff for data aggregation in wireless sensor networks under the physical interference model and using successive interference cancellation. We present theoretical lower bounds on both latency and energy as well as their tradeoff, and give an efficient approximation algorithm that can achieve the asymptotical optimum in both aggregation latency and latency-energy tradeoff. We show that our algorithm can significantly reduce the aggregation latency, for which the energy consumption is kept at its lowest possible level.

Index Terms—Data aggregation, latency-energy tradeoff, wireless sensor network, successive interference cancellation

1 Introduction

Wireless sensor networks have been extensively exploited for many environment monitoring applications in recent years. One of the core functions in these networks is data aggregation, which is to collect data from the wireless sensor nodes to deliver to a sink node. Typically, data aggregation is initiated by the sink using some SQL-like queries, such as "to find the highest temperature in the region." Messages generated at individual sensors carrying temperature data are first aggregated and processed at some relay sensors, for example, to derive the local maximum temperature; the locally processed results are further aggregated, and so on, until the final result reaches the sink. Besides the *max* function, other functions such as *min*, *sum*, *count*, and *average* can all be effectively implemented using data aggregation.

As the sensed data typically have a limited duration of validity, a fundamental requirement is that the total aggregation time, measured in time units and also referred to as the *aggregation latency*, must be minimized [1], [2], [3]. Additionally, the sensor nodes have to observe the hard constraint imposed by battery power and must strive for low energy consumption in each run of the data aggregation. Obviously, there exists some kind of tradeoff between aggregation latency and energy consumption (the *latency-energy tradeoff*) in wireless sensor data aggregation [4], [5], [6].

There have been some efforts to derive latency-energy tradeoff theoretically [7] as well as practical algorithms [4], [5], [6], which are all based on the *protocol interference model* (or equivalently the pairwise interference model). Under the protocol interference model, the transmission range and interference range of a node are simplified to two disks with radii r_t and $r_i(r_i \geq r_t)$, respectively. A transmission is successful if and only if the receiver lies within the transmission range of the sender and outside the interference range of any other concurrent sender. There has been, however, no prior study that is based on the *physical interference model* (or the cumulative interference model) which has been shown to be able to more accurately characterize the wireless interferences than the protocol interference model [8], [9], [10]. Designs based on the physical interference model can lead to increased network capacity. Under the physical interference model, the cumulative interference from all concurrent transmissions, for example, the $\sum_{e_j \in \Lambda_i} P_j/d_{ji}^{\alpha}$ part in (1), is taken into consideration at each receiver. A transmission along link e_i is successful if the *Signal-to-Interference-plus-Noise-Ratio (SINR)* at its receiver is above a certain threshold:

$$\frac{P_i/d_{ii}^{\alpha}}{N_0 + \sum_{e_j \in \Lambda_i} P_j/d_{ji}^{\alpha}} \geq \beta. \quad (1)$$

Here, Λ_i denotes the set of links that transmit simultaneously with e_i. P_i and P_j denote the transmission powers at the transmitter of link e_i and that of link e_j, respectively. $d_{ii}(d_{ji})$ is the distance between the transmitter of link e_i (e_j)

- *H. Li, C. Wu, D. Yu, and F.C.M. Lau are with the Department of Computer Science, The University of Hong Kong, Pokfulam Road, Hong Kong. E-mail: {hxli, cwu, dxyu, fcmlau}@cs.hku.hk.*
- *Q.-S. Hua is with the Institute for Theoretical Computer Science, Tsinghua University, Room 4-606-2 FIT Building, Beijing, P.R. China. E-mail: qshua@tsinghua.edu.cn.*

Manuscript received 3 Apr. 2012; revised 24 Sept. 2012; accepted 16 Oct. 2012; published online 29 Oct. 2012.
Recommended for acceptance by S. Papavassiliou.
For information on obtaining reprints of this article, please send e-mail to: tpds@computer.org, and reference IEEECS Log Number TPDS-2012-04-0346.
Digital Object Identifier no. 10.1109/TPDS.2012.314.

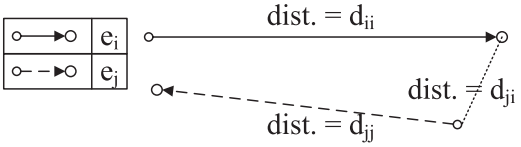

Fig. 1. An illustration of distances with two transmission links: e_i and e_j.

and the receiver of link e_i. Fig. 1 explains these distances graphically. α is the path loss ratio which has a typical value of between 2 and 6. N_0 is the ambient noise power. β is a positive constant as the *SINR* threshold for a successful transmission [3], [11].

With the physical interference model, a receiver can only successfully recover one signal from one sender in each time slot, among possibly several or many simultaneous transmissions. In recent years, it has been shown that, by applying *Multipacket Reception (MPR)* techniques [12], it is possible to break this one-time slot-one-sender barrier to let a receiver recover multiple individual signals from the mixed signal coming from multiple simultaneous senders. *Successive Interference Cancellation* (*SIC*), one subcategory of *MPR*, has been demonstrated practical by experimental study [13] implemented for the IEEE 802.15.4 [14] (ZigBee) physical layer, (a common physical-layer standard for sensor networks and other wireless personal area networks). The idea of *SIC* is to repeatedly identify the strongest signal and then remove (cancel) it from the mixed one using channel estimation, signal regenerating and subtraction [15]. To make it work, an interference cancellation sequence needs to be identified, such that for the ith signal to be canceled, the following criterion is satisfied:

$$\frac{P_i/d_{ii}^{\alpha}}{N_0+\sum_{e_j\in\Lambda_i-\Gamma_i}P_j/d_{ji}^{\alpha}+\sum_{e_k\in\Gamma_i,k\succ i}P_k/d_{ki}^{\alpha}}\geq\beta, \qquad (2)$$

where Γ_i is the set of concurrent transmission links connecting to the same receiver as e_is, and $k\succ i$ denotes that link e_i is canceled before link e_k. Extra energy is needed to recover the ith signal if it is not the last canceled one, to compensate for the cumulative interference from those links that are later canceled. Meanwhile, extra decoding delay, proportional to the number of canceled signals, is incurred for the entire signal cancellation process [13].

SIC techniques can potentially reduce the aggregation latency in wireless sensor networks significantly, because multiple transmissions can be scheduled in the same time slot while the saved scheduling latency may more than compensate for the incurred decoding delay (to be discussed in Section 3.2). Inevitably, the cost is increased energy consumption. To the best of our knowledge, there is no previous study that has tried to characterize the latency-energy tradeoff under SIC. Such characterization is needed to accurately gauge the practical benefits of applying SIC in typical wireless applications.

In this paper, we investigate the aggregation latency-energy tradeoff in wireless sensor networks under the physical interference model with successive interference cancellation. Our contributions are as follows:

▹ We prove a theoretical lower bound on the aggregation latency under the physical interference model with SIC: $\Omega(\max\{D,\log_{X+1}n\})$, where D is the network diameter in terms of the number of hops (the maximum of the minimum number of hops between any pair of nodes, when the nodes are transmitting using P_M and scheduled without mutual interference), n is the number of nodes, and $X=\lfloor\log_{1+\beta\frac{P_M}{N_0\beta}}+1\rfloor$ with P_M being the maximum transmission power of any node.

▹ We prove a theoretical lower bound, applicable to both the case with and that without SIC, on energy consumption under the physical interference model: $N_0\beta\frac{(n_{mis}d_M)^{\alpha}}{n^{\alpha-1}}$, where n_{mis} is the size of the maximum independent set with P_M (see Definition 1 in Section 4) of the given network and d_M is the maximum transmission range with maximum power P_M and zero interference.

▹ We prove a theoretical lower bound on the latency-energy tradeoff under the physical interference model with SIC that, for any aggregation algorithm, the product of the energy consumption approximation ratio and the $(\alpha-1)$th power of the aggregation latency approximation ratio is lower bounded by $\Omega(\Delta^{\alpha-1})$, where Δ is the maximum node degree (maximum number of nodes within the transmission range d_M of any node).

▹ We propose *EMA-SIC*, an *E*nergy-efficient *M*inimum-latency *A*ggregation algorithm under the physical interference model with SIC. As compared to existing work [3], [11] on minimum-latency data aggregation under the physical interference model, EMA-SIC can significantly lower the upper bound of the aggregation latency, to $O(D)$, and at the same time achieve an energy consumption approximation ratio that is the lowest possible with respect to the latency-energy tradeoff lower bound. In other words, our proposed algorithm achieves the asymptotical optimum in both aggregation latency and latency-energy tradeoff.

The remainder of the paper is organized as follows: We discuss related work in Section 2, and present the problem model in Section 3. We study the theoretical lower bounds for aggregation latency, energy consumption, and their tradeoff in Section 4. The EMA-SIC algorithm and its analysis are presented in Sections 5 and 6, respectively. The latency-energy efficiency of EMA-SIC is further studied via extensive simulations, the results of which are summarized and discussed in Section 7. Finally, we conclude the paper in Section 8.

2 Related Work

2.1 Minimum-Latency Data Aggregation

There is a large body of literature on data aggregation in wireless sensor networks [1], [2], [3], [11], [16], [17], [18], [19]. Most of the work target at minimum aggregation latency, without much consideration of the energy consumption. The current best upper bound on aggregation latency is $O(\Delta+R)$, which is based on the protocol interference model [1], [2], [16], [17], [18], where R is the network radius in hops and Δ is the maximal node degree.

The paper [1] is the first work that achieves the $O(\Delta+R)$ aggregation latency upper bound. In [2], the minimum-latency data aggregation problem in a multihop wireless sensor network with the assumption that each node has a unit transmission range and an interference range of $\rho\geq 1$

is studied. Xu et al. [17] propose an aggregation schedule based on a distributed algorithm, which achieves a guaranteed maximum aggregation latency of $16R + \Delta - 14$; they also prove a lower bound of $\max\{R, \log_2 n\}$ on the aggregation latency for any interference model, where n is the network size. Unlike the above work where connected dominating sets (CDSs) or maximal independent sets are employed, a novel approach of distributed aggregation with latency bound $O(\Delta + R')$ is introduced in [16], which is based on the idea of clustering. Here, R' is the inferior network radius satisfying that $R' \leq R \leq D \leq 2R'$ with D as the network diameter in hop-count. The *MLAS* problem is extended to the case with multiple sinks in [19] with latency bound of $O(\Delta + kR)$, where k is the number of sinks.

To the best of our knowledge, only two papers, [3] and [11], assume the physical interference model. A distributed aggregation scheduling algorithm with constant power assignment is proposed in [3], which achieves a latency upper bound of $O(\Delta + R)$. Li et al. [11] present a distributed algorithm with a latency bound of $O(K)$, where K is the logarithm of the ratio between the length of the longest link and that of the shortest link, and a centralized solution with an aggregation latency of $O(\log^3 n)$, which is the current best result among all proposed aggregation algorithms under the physical interference model. However, no limit on the power is assumed in [11].

2.2 Latency-Energy Tradeoffs in Data Aggregation

The existence of a tradeoff between energy consumption and aggregation latency in wireless sensor networks is widely recognized. There were some attempts targeting at efficient data aggregation algorithms with both low aggregation latency and low energy usage [4], [5], [6], [7], [20], but all are based on the protocol interference model expect [20], which only considers primary interference without mutual interference from other concurrent transmissions.

Yu et al. [4] explore the latency-energy tradeoff using techniques such as modulation scaling; algorithms are proposed to minimize the total energy consumption subject to a specified latency constraint. Arumugam and Kulkarni [5] propose a TDMA-based algorithm to effectively aggregate data in an energy-efficient way. In [6], the source node can specify its interest in minimizing energy consumption and/or source-to-sink delay, as input to the aggregation algorithm. The theoretical analysis in [7] demonstrates that there exists a latency-energy tradeoff in sensor data aggregation; an aggregation algorithm is designed, which achieves the asymptotical optimum for the tradeoff under the protocol interference model. To address the latency-energy tradeoff for in-network computation, of which data aggregation is a special case, an algorithm with order-optimal energy usage under given latency constraint is proposed in [20]. However, its order-optimality is derived over a network of uniformly random node distribution with simplified interference model as discussed previously, while not guaranteed over arbitrary network topologies.

To the best of our knowledge, there has been no work addressing the tradeoff under the physical interference model, let alone the case with arbitrary network topologies and/or SIC technique, which we address in this paper.

2.3 Successive Interference Cancellation

The techniques of successive interference cancellation have been exploited in recent years. Weber et al. [15] have analyzed the transmission capacity of wireless ad-hoc networks using SIC, with both upper bound and lower bound in closed form. Simeone et al. [21] analyze the capacity of linear two-hop mesh networks with SIC; a decode-and-forward relaying mechanism is proposed by exploiting the possible relevant intercell channel gains and rate splitting with SIC.

Wang and Garcia-Luna-Aceves [22] presented a polynomial-time heuristic algorithm to approximate the optimal network throughput in ad hoc networks with joint routing and scheduling using SIC. Lv et al. [23] proposed *simultaneity graph* to characterize the effect of SIC on link dependence due to interference, and presented an independent set-based greedy scheme to construct a maximal feasible schedule. Jiang et al. [24] advocated the use of joint SIC and interference avoidance and introduced a cross-layer optimization framework for the joint scheme. In [25], a SIC-based scheduling algorithm, with polynomial-time complexity, is proposed to find short schedules for networks with arbitrary distribution of nodes in the euclidean plane. However, none of the above considers the decoding delay with SIC. Our paper considers this issue.

3 The Problem Model

We consider a multihop wireless sensor network with n arbitrarily distributed sensor nodes $v_0, v_1, \ldots, v_{n-1}$ and a sink node v_n. The directed graph $G = (V, E)$ denotes the tree constructed for data aggregation from the sensor nodes to the sink, where $V = \{v_0, v_1, \ldots, v_n\}$ is the set of all nodes, and $E = \{e_0, e_1, \ldots, e_{n-1}\}$ is the set of transmission links in the tree with e_i representing the link from sensor node v_i to its parent. Without loss of generality, we assume that the minimum euclidean distance between each pair of nodes is 1.

We consider a time-slotted system. The transmission delay of one packet and the decoding delay to cancel one additional signal with SIC are normalized to 1 time unit and τ time unit, respectively. The actual length of any time slot t is $(1 + \chi_t \cdot \tau)$ time units, with χ_t being the maximum number of canceled signals at any scheduled receiver in this slot depending on whether the SIC technique is applied or not: $\chi_t = 0$ if there is no SIC application, and $\chi_t > 0$ otherwise.

3.1 The Data Aggregation Problem

The data aggregation problem is to use the links in E to construct a suitable tree and to design a correct and collision-free *aggregation schedule* $\mathcal{S} = \{S_0, S_1, \ldots, S_{T-1}\}$, where T is the total time slots for the schedule and S_t denotes the subset of links in E scheduled to transmit in time slot t, $t = 0, \ldots, T-1$. A *correct* aggregation schedule must satisfy the following conditions. First, any link should be scheduled exactly once, i.e., $\bigcup_{t=0}^{T-1} S_t = E$ and $S_i \cap S_j = \emptyset$, where $i \neq j$. Second, primary interference (that due to a node acting as a transmitter and a receiver in the same time slot) should be avoided; that is, $T(S_t) \cap R(S_t) = \emptyset, \forall t = 0, \ldots, T-1$, where $T(S_t)$ and $R(S_t)$ denote the transmitter set and receiver set for the links in S_t, respectively. Third, a nonleaf node v_i transmits to its parent only after all the links

TABLE 1
Notation Table

α	Path loss ratio, Sec. 1	D	Network diameter in terms of hop count, Sec. 1
β	*SINR* threshold, Sec. 1	n_{mis}	Size of maximum independent set, Sec. 1
N_0	Ambient noise power, Sec. 1	X	Max. cancelable signals at one receiver, Sec. 1
P_M	Max. transmission power, Sec. 1	χ_t	Max. canceled signals at each receiver, slot t, Sec. 3
d_M	Max. transmission range with P_M, Sec. 1	τ	Decoding delay to cancel one more signal, Sec. 3
Δ	Max. node degree, Sec. 1	h	Side length of hexagons, Sec. 5
n	Number of sensor nodes in network, Sec. 1	n_{cds}	Size of connected dominating set, Appendix I

in the subtree rooted at v_i have been scheduled, i.e., $T(S_i) \cap R(S_j) = \emptyset$ where $i < j$; in this way, v_i can conduct local process to aggregate all data from its subtree (e.g., local maximum temperature of its subtree) and transmits the aggregated data only once to save energy. An aggregation schedule is *collision-free* if each scheduled transmission in time slot t, i.e., $\forall e_i \in S_t$, can be correctly received by its receiver according to the interference model in Section 3.3, $\forall t = 0, \ldots, T-1$. Our objective is to minimize the aggregation latency, i.e., the overall time units of all slots, as well as the latency-energy tradeoff. Note that the aggregation latency already includes the end-to-end transmission delay, decoding delay with SIC, and the cumulative queuing delay, because it is defined as the time span between the time-point of first transmission and that when the sink collects all data.

3.2 Decoding Delay with SIC

With the SIC technique for the ZigBee standard in [13], one packet typically has a length of 128 bytes, which are modulated into 4,096 physical-layer symbols. Symbols of each signal are decoded and canceled sequentially, with the requisite that three consecutive symbols should be buffered for each canceled symbol. The decoding delay for each canceled signal is the time span for three symbols, which is $\tau = \frac{3}{4{,}096}$ of the transmission delay. If we have χ_t signals to cancel out, the total decoding delay is $\frac{3\chi_t}{4{,}096}$ time units while the saved transmission delay is χ_t time units, i.e., one time unit for each canceled signal. Thus, SIC has great potential in reducing the aggregation latency in wireless sensor networks. The above setting for decoding delay is also applied in our simulation study as described in Section 7.

3.3 Interference and Energy Models

We adopt the *physical interference model* with the application of *successive interference cancellation*. With SIC, a receiver can recover multiple signals from simultaneous transmitters from the mixed signal received, as long as an interference cancellation sequence of the signals can be determined. The sequence is such that the ith signal remains strong enough, as judged by condition (2), after the previous $i-1$ signals have been removed (canceled) from the mixed signal. If SIC is not applied at a receiver, the receiver can recover at most one signal (from one sender) in each time slot, subject to condition (1).

In our study, we use the energy model that the power attenuation along each transmission link of length r is proportional to r^α, $\alpha \geq 2$, i.e., the received power is P/r^α if the sender uses transmission power P.

Let P_i denote the transmission power used by node $v_i, i = 0, \ldots, n-1$, and the maximum transmission power at any sensor node be P_M.[1] We assume no isolated node, i.e., each node can transmit to at least one other node in the network if the power level of P_M is used. Let D be the network diameter, which is in hops instead of the geometric distance, and is defined as the maximum of the minimum number of hops between any pair of nodes when the nodes are transmitting using maximum power P_M; and d_M be the maximum transmission range of a node when using P_M with zero interference.

Important notations used in the paper are summarized in Table 1 with descriptions and places of first appearances.

4 Theoretical Lower Bounds

We first investigate the theoretical lower bounds on the aggregation latency, the energy consumption, and the latency-energy tradeoff for the data aggregation problem, respectively.

4.1 Energy Consumption Bound

We prove in Theorem 1 a lower bound, applicable to both the case with and that without SIC, on the overall energy consumption for data aggregation under the physical interference model.

Definition 1 (Maximum Independent Set with P_M). *An independent set with P_M in a wireless sensor network G is a subset of nodes in the network graph, such that no node in the set can successfully transmit to another node in the set using the maximum power P_M with zero interference, and a maximum independent set with P_M is the largest such independent set in the graph, i.e., it has the maximum number of nodes.*

Theorem 1 (Energy Consumption Lower Bound). *Suppose the size of the maximum independent set with P_M containing the sink in a wireless sensor network is $n_{mis}+1$. The overall energy consumption for data aggregation in the network under the physical interference model, with or without SIC, is lower-bounded by $N_0\beta\frac{(n_{mis}d_M)^\alpha}{n^{\alpha-1}}$.*

We prove Theorem 1 by analyzing the energy consumption when links are scheduled in a "TDMA" fashion, i.e., only one link is scheduled to transmit in each time slot, and the data aggregation tree is a minimum spanning tree (MST) of the network, of which the weight of link e_i is d_{ii}^α, where d_{ii} is the euclidean length of link e_i. A Theorem from [26] is also utilized for the proof with more details in

1. We consider homogeneous networks with identical maximum transmission power on each node.

Appendix A, which can be found on the Computer Society Digital Library at http://doi.ieeecomputersociety.org/10.1109/TPDS.2012.314. Appendices B-K can also be found at this link.

4.2 Aggregation Latency Bound

In their recent work, Xu et al. [17] give a latency lower bound of $\Omega(D+\Delta)$ on sensor data aggregation under the protocol interference model, and a latency lower bound of $\Omega(\max\{R, \log_2 n\})$ under any interference model. We next prove an aggregation latency lower bound under the physical interference model with SIC.

Theorem 2 (Aggregation Latency Lower Bound). *The latency of data aggregation in a wireless sensor network under the physical interference model with SIC, is lower bounded by* $\Omega(\max\{D, \log_{X+1} n\})$, *where* $X = \lfloor \log_{1+\beta} \frac{P_M}{N_0\beta} + 1 \rfloor$.

We first demonstrate that X is the maximum cancelable signals at one receiver, and then prove Theorem 2 by showing that the aggregation latency lower bound is achieved using maximum transmission power with D, n, and X as dominant factors. Detailed proof is in Appendix B, available in the online supplemental material.

4.3 Latency-Energy Tradeoff

The lower bounds on aggregation latency and overall energy consumption, as just derived, may not be achievable concurrently: the lower bound on energy consumption given in Theorem 1 is achieved only when the aggregation tree is a minimum spanning tree of the network and exactly one transmission along the tree is scheduled in each time slot. In this case, the aggregation latency is n. On the other hand, to achieve the lower bound on aggregation latency of $\Omega(\max\{D, \log_{X+1} n\})$ as given in Theorem 2, larger powers up to P_M at the transmitters may need to be used. Consequently, the tradeoff between aggregation latency and energy consumption needs to be addressed in the design of any data aggregation algorithm, which is the main objective of this paper.

Theorem 3 presents a theoretical lower bound on the combined performance of aggregation latency and energy consumption. The theorem is not to establish a definition for the latency-energy tradeoff, which may vary with different application concerns. However, the result in Theorem 3 can serve as a metric to examine whether an algorithm has achieved the best it can do in terms of both aggregation latency and energy consumption, with a tradeoff in between. A similar metric can be found in [7] under the protocol interference model.

Theorem 3 (Latency-Energy Tradeoff Lower Bound). *Let* ρ_L *and* ρ_E *denote the approximation ratios of the aggregation latency and energy consumption with regard to the lower bounds in Theorems 1 and 2, respectively, with any given data aggregation algorithm. The product of the energy consumption approximation ratio, i.e.,* ρ_E, *and the* $(\alpha-1)$*th power of the aggregation latency approximation ratio, i.e.,* $\rho_L^{\alpha-1}$, *is lowered-bounded by* $\Omega(\Delta^{\alpha-1})$ *in wireless networks under the physical interference model with SIC.*

To prove the theorem, we show that there exists a sample network of $n+1$ nodes with maximum node degree Δ such that $\rho_L^{\alpha-1}\rho_E$ is lowered bounded by $\Omega(\Delta^{\alpha-1})$ under the physical interference model with SIC. See more details in Appendix C, available in the online supplemental material.

We will show in Section 6 that our algorithm, to be proposed in Section 5, is asymptotically optimal in both aggregation latency and latency-energy tradeoff, with respect to the lower bounds in Theorems 1, 2, and 3.

5 EMA-SIC: Energy-Efficient Minimum-Latency Data Aggregation Algorithm with Successive Interference Cancellation

We now design our *EMA-SIC algorithm*, which can outperform any other existing algorithm by its reduced maximum aggregation latency and asymptotically optimal latency-energy tradeoff. It uses the successive interference cancellation technique, and consists of two parts: tree construction (T) and link scheduling (S).

5.1 Tree Construction with *SIC*

The aggregation tree construction in EMA-SIC comprises three steps, executed in a distributed fashion:

T1. Breadth-first search is launched by the sink v_n to find a spanning tree of the network rooted at it, based on maximum transmission ranges of the nodes. Each node is assigned a level, indicating its hop-count to the sink. The sink node is initialized with level 0.

T2. A connected dominating set (CDS) of the network (see Definition 2) is identified in the breath-first spanning (BFS) tree, by treating the sink as the first dominator and then finding other dominators using the most widely adopted algorithm, which is distributed, in [26]. This algorithm is executed in two phases to find the connected dominating set. In the first phase, a maximum independent set is constructed such that the distance between any pair of its complementary subsets is exactly two hops. Based on the constructed MIS, the second phase generates a connected dominating set by strategically selecting nodes to be added to or removed from the MIS. A tree rooted at the sink and connecting all other nodes in the connected dominating set can be built, such that each node in level $l \geq 1$ connects to its parent node in level $l-1$ of the BFS tree.

Definition 2 (Connected Dominating Set with P_M). *A dominating set with* P_M *in a wireless sensor network* G *is a subset of nodes in the graph, such that every node outside the set can successfully transmit to at least one node in the set using the maximum power* P_M. *The nodes in a dominating set are referred to as dominators, and those not in the set are dominatees. A connected dominating set with* P_M *is a dominating set within which any node can transmit to at least another node using* P_M.

T3. This step consists of two phases. Consider the dominators in the connected dominating set derived in the previous step. In the first phase, i.e., step T3.a, each dominator finds a disk centered at itself with radius equal to the maximum transmission range d_M, and use equal-sized hexagons to cover the disk. An example is given in Fig. 2a. The side length of the hexagons is $h = \min\{d_1, d_2\}$ with

$$d_1 = \frac{-1 + \sqrt{1 + 4/3(1 + \log_{1+\beta} \sqrt{P_M/(N_0\beta)})}}{2}$$

and $d_2 = \frac{1}{2}(\frac{P_M}{N_0\beta})^{\frac{1}{2\alpha}}$, which are carefully assigned to ensure the validness of our algorithm, i.e., $K_1 > 0$ which is a parameter to be introduced shortly, proven in Appendix D, available

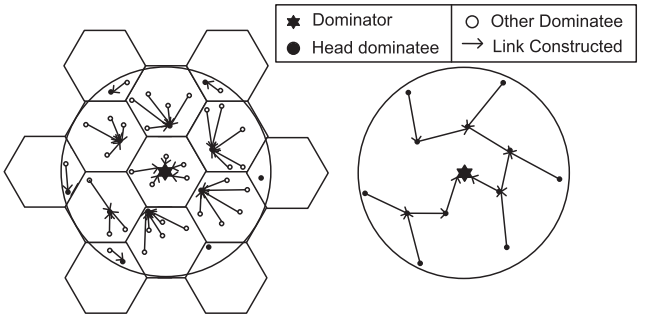

Fig. 2. The third step of tree construction in EMA-SIC: an example with one dominator.

in the online supplemental material. In each hexagon, the dominatee which is closest to the dominator is chosen as the *head* dominatee. We prove in Section 6 that, with our assignment of the hexagon side length, all dominatee nodes in a hexagon can concurrently transmit to the head dominatee, which can successfully recover these transmissions using successive interference cancellation.

Note that each dominator only needs the location information of the dominatees within the disk as in Fig. 2. Besides, the relative coordinate (x, y) of each dominatee to its dominator at the origin $(0, 0)$ is adequate to decide which hexagon it resides in and whether it is the head dominatee, without the use of absolute coordinates in the global view. So step T3a can be executed in a fully distributed fashion on each dominator with just the relative locations of its dominatees.

In the next phase, i.e., step T3.b, for the much sparser topology consisting of only the head dominatees and the dominators, a local minimum spanning tree is built to connect the head dominatees to each dominator, as shown in Fig. 2b. In constructing the MST, a link with length r has weight r^α, which reflects the power attenuation along the link. Using the connected dominating set as the backbone, a data aggregation tree of the entire network is formed.

In the above procedure, if a dominatee happens to reside in the overlapping area of hexagons or disks belonging to different dominators, it chooses to join the tree construction of the dominator that is geometrically closest to the sink.

Fig. 12 in Appendix E, available in the online supplemental material, illustrates the tree construction procedure with an example.

5.2 Link Scheduling with *SIC*

The aggregation schedule consists of three steps: (S1) schedule the transmissions in individual hexagons from the nonhead dominatees to the head dominatee; (S2) schedule the transmissions from head dominatees to their dominators along the local minimum spanning trees; and (S3) schedule the aggregation transmissions of the dominators along the tree connecting them to the sink.

For step S1, within each hexagon, all the nonhead dominatees transmit concurrently to the head dominatee. In order for the head dominatee to recover all the transmissions correctly, the transmission power for the ith link in the cancellation sequence, which has a link length of d_{ii}, is assigned to be $(N_0 + I)\beta(1+\beta)^{X'-i} d_{ii}^\alpha$, where $I = \frac{P_M/(2h)^\alpha}{\beta(1+\beta)^{X'-1}} - N_0$ is the upper bound of the cumulative interference from current transmissions in other hexagons and $X' = 3h^2 + 3h$ is the maximum number of nonhead dominatees in any hexagon. The detailed derivation of I, X', and the power assignment can be found in the proof of Theorem 4 in Section 6 to show the correctness of EMA-SIC.

To alleviate interhexagon interferences, a schedule of hexagons is designed following the rule that the head dominatees in any two hexagons, of which the transmissions are scheduled in the same time slot, should be separated by a distance of greater than $K_1 + 1$ times the maximum link length $2h$ in a hexagon, where

$$K_1 = (6X')^{\frac{1}{\alpha}} \left(1 + \left(\frac{2}{\sqrt{3}}\right)^\alpha \frac{1}{\alpha - 2}\right)^{\frac{1}{\alpha}} \times \left(\frac{1}{\beta(1+\beta)^{X'-1}} - \frac{N_0(2h)^\alpha}{P_M}\right)^{-\frac{1}{\alpha}}.$$

To achieve collision-free link scheduling in steps S2 and S3, we apply the following two rules: 1) any two concurrent transmitters should be separated by a distance of at least $(K_2 + 1)d_M$, with $K_2 = (6\beta(1 + (\frac{2}{\sqrt{3}})^\alpha \frac{1}{\alpha-2}) + 1)^{1/\alpha}$, to bound the cumulative interference at each receiver; 2) the transmission power for a link of length r is set to $N_0\beta(2 - 1/K_2^\alpha)r^\alpha$. This idea of separating concurrent transmitters by a predefined distance was also employed in [27], which, however, did not consider background noise in the interference model (we do here).

Note that, similar approaches of covering the network with hexagons are also utilized in aggregation algorithms of [3] and [11], but with fundamental differences from ours in following ways: 1) in [3], the network is covered with equal-sized grids just for link scheduling across different grids without contribution to tree construction while our application of hexagons both constructs the aggregation tree and schedules link transmissions within the same hexagon; 2) in [11], hexagons with differentiated sizes are iteratively used to construct the tree but with unlimited power assignment while our paper shows practical concern with maximum transmission power and applies hexagons with unique sizes for only part of the tree construction; moreover, absolute locations of all nodes in the global view are required in [11] while our paper just needs a weaker condition of relative position of each dominatee to its dominator.

The EMA-SIC algorithm is summarized in Algorithm 1.

Algorithm 1. *EMA-SIC* Algorithm.
Input: Node set V and the sink node v_n.
Output: Aggregation tree E and link schedule S.
1: Initialization: $E, S \leftarrow \emptyset$.
2: Step T1: Construct a BFS tree on V rooted at v_n.
3: Step T2: Construct a CDS on the BFS tree which includes v_n; build a spanning tree of the dominators rooted at v_n; add tree links to E.
4: Step T3.a: Cover the network with hexagons and connect each non-head dominatee to its head dominatee in the hexagon; add links to E.
5: Step T3.b: For each dominator, construct a local MST of its head dominatees rooted at it; add tree links to E.

6: $d_1 := \frac{-1+\sqrt{1+4/3(1+\log_{1+\beta}\sqrt{P_M/(N_0\beta)})}}{2}$; $d_2 := \frac{1}{2}\left(\frac{P_M}{N_0\beta}\right)^{\frac{1}{2\alpha}}$;
$h := \min\{d_1, d_2\}$; $X' := 3h^2 + 3h$; $I := \frac{P_M/(2h)^\alpha}{\beta(1+\beta)^{X'-1}} - N_0$;
$K_1 := (6X')^{\frac{1}{\alpha}}\left(1 + \left(\frac{2}{\sqrt{3}}\right)^\alpha \frac{1}{\alpha-2}\right)^{\frac{1}{\alpha}}\left(\frac{1}{\beta(1+\beta)^{X'-1}} - \frac{N_0(2h)^\alpha}{P_M}\right)^{-\frac{1}{\alpha}}$.

7: Step S1: Schedule transmissions in hexagons from non-head dominatees to their head dominatees, such that any two concurrent receivers are separated by at least $2(K_1+1)h$, and the transmission power is $(N_0+I)\beta(1+\beta)^{X'-i}d_{ii}^\alpha$ for the i^{th} link in the receiver's cancellation sequence with length d_{ii}; add schedule to S.

8: $K_2 := \left(6\beta\left(1 + \left(\frac{2}{\sqrt{3}}\right)^\alpha \frac{1}{\alpha-2}\right) + 1\right)^{1/\alpha}$.

9: Steps S2 & S3: Schedule the link transmissions in the aggregation tree containing only head dominatees and dominators, such that any two concurrent transmitters are separated by at least $(K_2+1)d_M$ and transmission power is $N_0\beta(2 - 1/K_2^\alpha)r^\alpha$ for a link of length r; add the schedule to S.

10: **return** E and S

6 Analysis of *EMA-SIC*

We next prove the correctness, as well as the latency and energy efficiencies of our algorithm.

6.1 Correctness

Theorem 4 (Correctness of *EMA-SIC*). *EMA-SIC constructs a data aggregation tree and achieves a correct and collision-free aggregation schedule under the physical interference model.*

Proof Sketch. It is easy to see an aggregation tree rooted at the sink is correctly constructed from the tree construction algorithm in EMA-SIC. We prove that EMA-SIC achieves a correct and collision-free aggregation schedule (see Section 3.1) by presenting upper bounds for cumulative interferences at each receiver in each step of the link scheduling (a theorem from [31] is applied), and showing that each received signal in step S1 and in steps S2 and S3 of the link scheduling satisfies the SINR constraint in (2) and (1) even with its corresponding upper bound of cumulative interferences, respectively. The detailed proofs can be found in Appendices F and G, available in the online supplemental material, respectively. □

6.2 Energy and Latency Efficiencies

We show that EMA-SIC outperforms any other algorithm as it can reduce the maximum aggregation latency to $O(D)$, while maintaining an energy consumption approximation ratio that is the lowest possible—$O(\Delta^{\alpha-1})$.

Theorem 5 (Latency Efficiency with *EMA-SIC*). *The aggregation latency with EMA-SIC in any given network with network diameter D is upper bounded by $O(D)$, and the aggregation latency approximation ratio (with respect to the lower bound in Theorem 2) is upper bounded by $O(1)$.*

We prove Theorem 5 by showing that the scheduling latencies for step S1 and S2 are bounded with constant values while step S3 has an upper-bounded latency in the order of $O(D)$. See detailed proof in Appendix H, available in the online supplemental material.

Theorem 6 (Energy Efficiency with *EMA-SIC*). *The energy consumption approximation ratio, that is, the upper bound of the overall energy consumption with using EMA-SIC to the lower bound in Theorem 1, is upper bounded by $O(\Delta^{\alpha-1})$, in any given network with a maximum node degree of Δ.*

To prove Theorem 6, the upper bounds of energy consumption for steps S1, S2, and S3 are analyzed and characterized with n_{mis}, respectively. A theorem from [32] is applied, with detailed proof in Appendix I, available in the online supplemental material.

The following corollary shows that the energy consumption approximation ratio in Theorem 6 is indeed tight, for any algorithm achieving the aggregation latency upper bound in Theorem 5.

Corollary 1 (Asymptotic optimum with *EMA-SIC*). *The aggregation latency and the latency-energy tradeoff with EMA-SIC in any given network are asymptotically optimal, or equivalently, with $O(1)$ approximation ratios with respect to the lower bounds in Theorems 1, 2 and 3.*

This corollary can be easily proved by checking the approximation ratios of aggregation latency and energy consumption of *EMA-SIC* in Theorems 5 and 6, as well as the latency-energy tradeoff lower bound in Theorem 3.

Comparing our analytical results in Theorems 5 and 6 with those in [11] and [3], we can see that EMA-SIC reduces the upper bound of the maximum aggregation latency to $O(D)$ (which is the current best result in literature), and at the same time achieves an approximation ratio of energy consumption that is the lowest possible (Corollary 1).

7 Simulation Results

We have presented the asymptotic performance of EMA-SIC in terms of aggregation latency and energy consumption together with their tradeoff by analyzing the respective upper bounds and approximation ratios in the worst cases. In this section, we further investigate the latency-energy efficiencies of EMA-SIC in average cases by comparison with two distributed aggregation algorithms under the physical interference model: Li et al.'s algorithm in [3] and the Cell-AS algorithm in [11].

We conducted our simulation in the *Sinalgo* [28] simulation framework, a packet-level wireless network simulator for testing and validating network algorithms.

Using a setting similar to that in [11], we consider wireless sensor networks having 100 to 1,000 nodes that are randomly distributed with *Uniform*, *Poisson* or *Cluster* distributions[2] in a square field with side length from 100 to 200 meters.[3] Fig. 14 in Appendix J, available in the online supplemental material, gives an illustration of network topologies with 100 nodes under different distributions. The power of the background noise N_0 is set to a constant 10^{-6} joule/time unit. Since the path loss ratio α has a typical

2. Please refer to [11] for a detailed explanation of each distribution.
3. With a given number of nodes in the network, varying the network scale will change the node density.

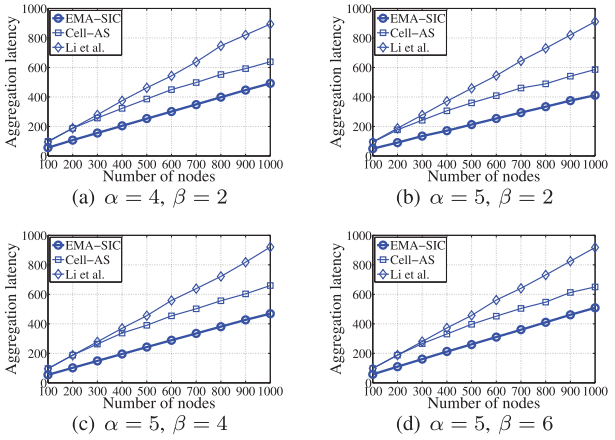

Fig. 3. Aggregation latency (time units) comparison under selected network settings in a 200×200 m^2 area.

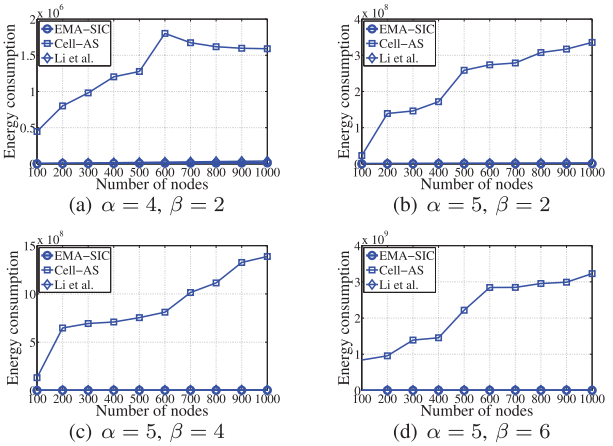

Fig. 4. Energy consumption (joule) comparison under selected network settings in a 200×200 m^2 area.

value between 2 and 6 and the SINR threshold β is generally assumed to be larger than 1 [3], [11], α is assigned 3, 4, and 5 in the various settings, while β is set to 2, 4, 6 and 10, 15, 20 for the low SINR and high SINR scenarios, respectively. The maximum transmission powers for Li et al.'s algorithm and the EMA-SIC algorithm are assigned values that would result in a transmission range of 40 meters and can maintain the network connectivity with high probability.[4] The maximum transmission power in Cell-AS algorithm is infinite since no power limitation is assumed [11]. The decoding delay with SIC is calculated as in Section 3.2. Each datum is an average of 100 trials.

Li et al.'s algorithm is only effective with uniform node distribution, network side length of 180 and 200, and (α, β) being the pairs $(4, 2)$, $(5, 2)$, $(5, 4)$, and $(5, 6)$, consistent with the report in [11].

We, therefore, compare the latency-energy performance of the three algorithms under those settings in Figs. 3, 4, 5, 6, 7, 8, 9, and 10. Complete simulation results with other node distributions, network side lengths, and (α, β) value pairs can be found our technical report [29], due to space constraint.

7.1 Aggregation Latency and Energy Consumption

Figs. 3, and 4[5] show that EMA-SIC outperforms both the Cell-AS and Li et al.'s algorithms in aggregation latency in all cases, while consuming similar levels of energy as Li et al.'s algorithm (their curves largely overlap in Fig. 4; they will be compared separately in Fig. 5), which are far lower than those of the Cell-AS algorithm. The high energy consumption of the Cell-AS algorithm results from its assumption of unlimited transmission power [11].

Fig. 4 also shows that the energy consumption of Cell-AS may go down when the number of nodes reaches 700-1,000, which can be explained by the decrease of link lengths between nodes (thus decreased transmission power per link) when the node density in the same square area increases.

4. Disconnected networks are meaningless in our problem since the sink cannot receive the data from all sensor nodes.

5. Results with network side length 180 under similar settings as in Figs. 3, 4, 5, 6, and 7 can be found in Appendix K, available in the online supplemental material.

As stated previously, it is hard to tell the differences between the energy consumption curves of EMA-SIC and Li et al.'s algorithm in Fig. 4. Thus, we conduct a separate comparison of energy usage just between EMA-SIC and Li et al.'s algorithm, and show that EMA-SIC is superior to Li et al.'s algorithm in energy consumption in Fig. 5. The curves of Li et al.'s algorithm are straight lines in Fig. 5 as a result of its constant power assignment [3].

Another observation with Figs. 3, 4, and 5 is that: 1) the aggregation latency of each algorithm is lower in settings with larger α (which means more path loss of power, and thus lower interference from other nodes) and smaller β (corresponding to lower SINR requirement); 2) the energy consumption of each algorithm increases with the enhanced value of α (requiring higher transmission power to counteract the increased power loss and to meet the SINR requirement) and β (higher SINR requirement).

7.2 Latency-Energy Tradeoff

Next, we adopt the metric for latency-energy tradeoff of "the product of energy consumption and the $(\alpha - 1)$th power of aggregation latency" to examine the performance of these algorithms in Fig. 6 for selected settings. The metric

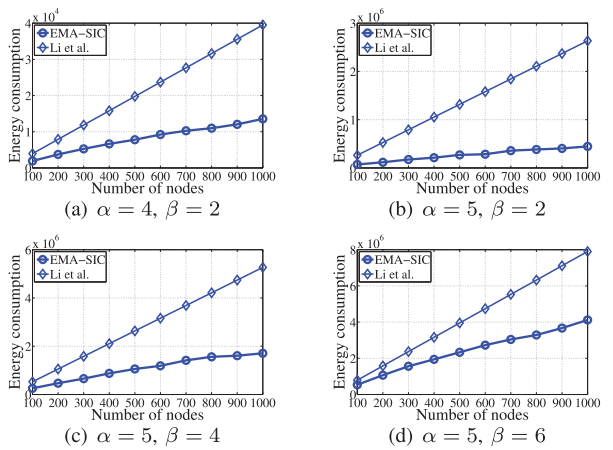

Fig. 5. A separate comparison of energy consumption (joule) between EMA-SIC and Li et al.'s algorithm under selected network settings in a 200×200 m^2 area.

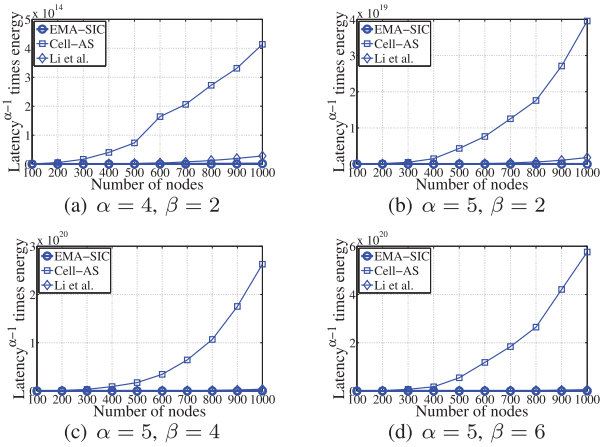

Fig. 6. Latency-energy tradeoff comparison under selected network settings in a $200 \times 200\ \mathrm{m}^2$ area.

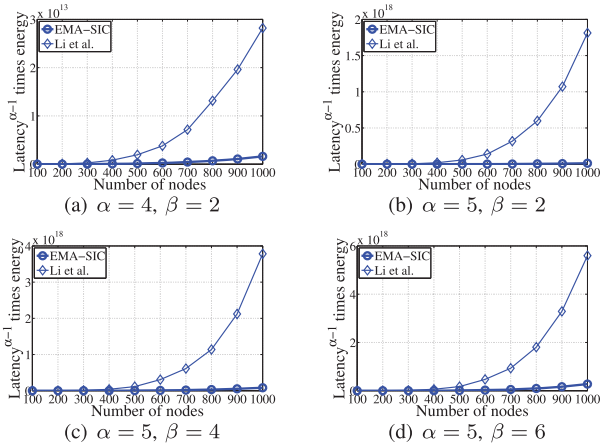

Fig. 7. A separate comparison of latency-energy between EMA-SIC and Li et al.'s algorithm under selected network settings in a $200 \times 200\ \mathrm{m}^2$ area.

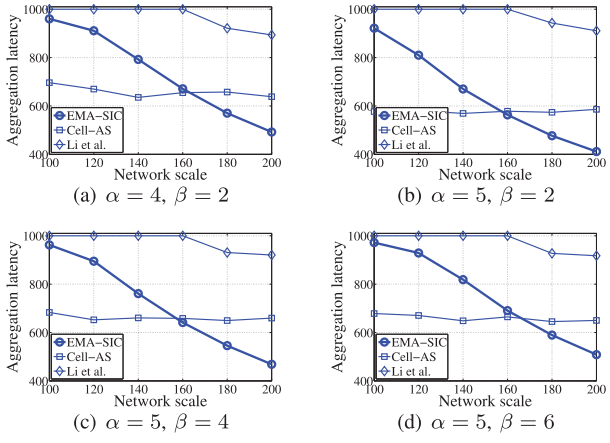

Fig. 8. Impact of network scale on the aggregation latency (time units) under selected network settings with uniform distribution and 1,000 nodes.

proposed in Theorem 3 is equal to this revised metric divided by "the product of the optimal energy consumption and the $(\alpha - 1)$th power of the optimal aggregation latency." Since the optimums of both aggregation latency and energy consumption of a given network should be the same for any aggregation algorithm, while the optimal aggregation latency of any given network is hard to find

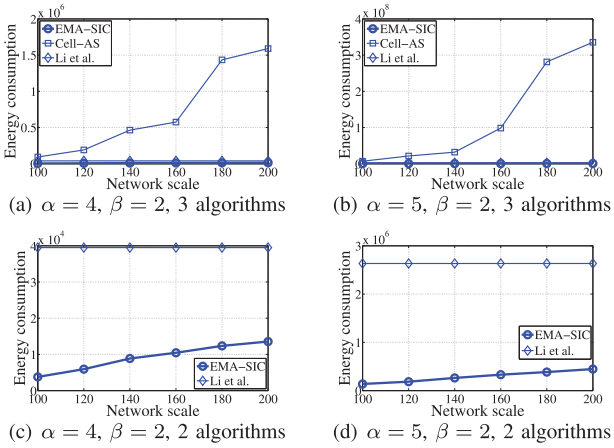

Fig. 9. Impact of network scale on the energy consumption (joule) under selected network settings with uniform distribution and 1,000 nodes.

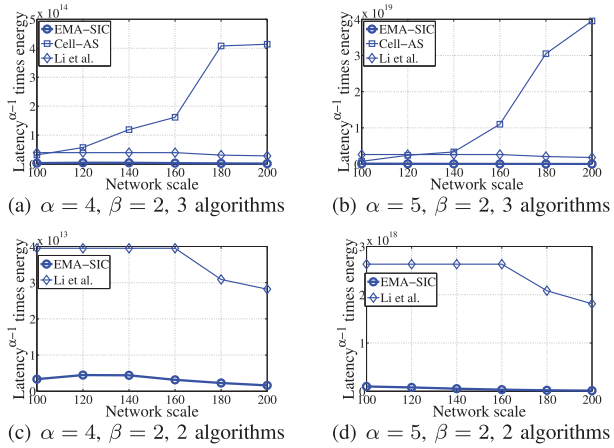

Fig. 10. Impact of network scale on the latency-energy tradeoff under selected network settings with uniform distribution and 1,000 nodes.

under the physical interference model (NP-hard), we adopt the revised metric here, which is equivalent to the previous metric multiplied by a constant factor.

It can be observed that the Cell-AS algorithm has a significantly poorer latency-power tradeoff if compared with that of the other two algorithms. As the performance differences for Li et al.'s algorithm and the EMA-SIC algorithm are not distinguishable in Fig. 6, we present a separate comparison of latency-energy tradeoff between these two algorithms in Fig. 7. We can see that EMA-SIC algorithm achieves an evidently better latency-energy tradeoff, further confirming its superiority to other aggregation algorithms.

7.3 Impact of Network Scale

We also examine the impact of network scale on the latency-energy efficiency of the three algorithms under various network settings. Note that because the network topologies are generated randomly, it is not that straightforward to adjust the network diameter or node degree for performance comparison. Thus, we indirectly change the network diameter and node degree by varying the network scale. With the same number of nodes in the network, increasing the network scale will result in increased average network diameter and decreased average node degree.

We present results under selective settings in which Li et al.'s algorithm would put forth its effectiveness, in Figs. 8, 9, and 10 with uniformly distributed 1,000 nodes. Detailed comparisons under other settings are included in technical report [29].

In Fig. 8, we see that: 1) Li et al.'s algorithm becomes effective when network scale reaches 180×180 square meters (detailed explanation in [11]); 2) the Cell-AS algorithm has a relatively stable latency performance when network scale varies, which is due to its assumption of unlimited transmission power such that the network diameter and maximum node degree are fixed as 1 and n, respectively; and 3) the latency with EMA-SIC keeps decreasing when the size of network scales up (larger network diameter and smaller node degree), which can be understood as that larger network scale leads to smaller node density and, thus, lower mutual interference among node pairs and more collision-free scheduling opportunities. Network diameter is the dominant factor for worst-case study to find theoretical bounds for aggregation latency as in Sections 4 and 6. But, the impact of node degree overwhelms the network diameter on the average latency performance in random cases.

Although Cell-AS performs better, in aggregation latency, than EMA-SIC when the network scale is smaller than 160×160 square meters, we argue that the impractical assumption of unlimited power by the Cell-AS algorithm will render it unapplicable in power-constraint cases (wireless sensor networks typically belong to these cases). In contrast, EMA-SIC fits well in all network settings, with any given maximum transmission power. Besides, EMA-SIC strictly outperforms Cell-AS in energy consumption and latency-energy tradeoff as shown in Figs. 9 and 10.

In Figs. 9 and 10, we present the simulation results for $(\alpha, \beta) \in \{(4,2),(5,2)\}$ while that for $(\alpha, \beta) \in \{(5,4),(5,6)\}$ are similar and are included in Appendix K, available in the online supplemental material, due to space constraint. With Figs. 9a and 9b, we have that the Cell-AS algorithm consumes much higher energy, proportional to the network scale, than the others, which is a consequence of its unlimited power assumption. In Figs. 9c and 9d, we conduct a separate comparison of energy consumption between EMA-SIC and Li et al.'s algorithm. We can see that: 1) Li et al.'s algorithm has the same energy consumption in various network scales as a result of its constant power assignment; and 2) EMA-SIC consumes significantly lower energy, also proportional to the network scale (which is a natural result because of the increased distances among node pairs in networks with larger scale). Figs. 10a and 10b present the latency-energy tradeoff by the three algorithms. Cell-AS algorithm has the poorest tradeoff performance, which scales up with the network side length, while Figs. 10c and 10d demonstrate that the EMA-SIC algorithm also remarkably outperforms Li et al.'s algorithm in latency-energy tradeoff.

8 Concluding Remarks

This paper investigates the latency-energy tradeoff of data aggregation in wireless sensor networks under the physical interference model and using the successive interference cancellation technique. We derive the theoretical lower bounds on both aggregation latency and energy consumption as well as their tradeoff, and give an energy-efficient minimum-latency data aggregation algorithm (EMA-SIC), which can achieve the asymptotically optimal aggregation latency and latency-energy tradeoff. We show that the EMA-SIC algorithm has a constant approximation ratio of aggregation latency (with respect to the theoretical lower bound) while consuming the lowest possible amount of energy. We conduct simulation studies to further validate the superiority of EMA-SIC in terms of latency-energy performance over other work under the physical interference model. As our ongoing work, we plan to evaluate the latency-energy tradeoff in wireless sensor networks with dynamics, for example, stochastic node sleep and wake up events, and heterogeneous node capabilities, for example, differentiated battery power.

References

[1] S.C.H. Huang, P. Wan, C.T. Vu, Y. Li, and F. Yao, "Nearly Constant Approximation for Data Aggregation Scheduling in Wireless Sensor Networks," *Proc. IEEE INFOCOM '07,* 2007.

[2] P.J. Wan, S.C.H. Huang, L.X. Wang, Z.Y. Wan, and X.H. Jia, "Minimum-Latency Aggregation Scheduling in Multihop Wireless Networks," *Proc. ACM MOBIHOC '09,* 2009.

[3] X.Y. Li, X.H. Xu, S.G. Wang, S.J. Tang, G.J. Dai, J.Z. Zhao, and Y. Qi, "Efficient Data Aggregation in Multi-Hop Wireless Sensor Networks under Physical Interference Model," *Proc. IEEE Sixth Int'l Conf. Mobile Ad Hoc and Sensor Systems (MASS '09),* 2009.

[4] Y. Yu, B. Krishnamachari, and V.K. Prasanna, "Energy-Latency Tradeoffs for Data Gathering in Wireless Sensor Networks," *Proc. IEEE INFOCOM '04,* 2004.

[5] M. Arumugam and S.S. Kulkarni, "Tradeoff between Energy and Latency for Converge Cast," *Proc. IEEE Second Int'l Workshop Networked Sensing Systems (INSS '05),* 2005.

[6] H.M. Ammari and S.K. Das, "Trade-Off between Energy Savings and Source-to-Sink Delay in Data Dissemination for Wireless Sensor Networks," *Proc. ACM Eighth ACM Int'l Symp. Modeling, Analysis and Simulation of Wireless and Mobile Systems (MSWiM '05),* 2005.

[7] X.Y. Li, Y. Wang, and Y. Wang, "Complexity of Data Collection, Aggregation, and Selection for Wireless Sensor Networks," *IEEE Trans. Computers,* vol. 60, no. 3, pp. 386-399, Mar. 2011.

[8] G. Brar, D. Blough, and P. Santi, "Computationally Efficient Scheduling with the Physical Interference Model for Throughput Improvement in Wireless Mesh Networks," *Proc. ACM MOBICOM '06,* 2006.

[9] D. Chafekar, V.S. Kumar, M.V. Marathe, S. Parthasarathy, and A. Srinivasan, "Approximation Algorithms for Computing Capacity of Wireless Networks with SINR Constraints," *Proc. IEEE INFOCOM '08,* 2008.

[10] T. Moscibroda, "The Worst-Case Capacity of Wireless Sensor Networks," *Proc. ACM/IEEE Sixth Int'l Symp. Information Processing in Sensor Systems (IPSN '07),* 2007.

[11] H. Li, Q.-S. Hua, C. Wu, and F.C.M. Lau, "Minimum-Latency Aggregation Scheduling in Wireless Sensor Networks Under Physical Interference Model," *Proc. ACM 13th ACM Int'l Conf. Modeling, Analysis, and Simulation of Wireless and Mobile Systems (MSWiM '10),* 2010.

[12] J. Andrews, "Interference Cancellation for Cellular Systems: A Contemporary Overview," *IEEE Wireless Comm.,* vol. 12, no. 2, pp. 19-29, Apr. 2005.

[13] D. Halperin, T.E. Anderson, and D. Wetherall, "Taking the Sting Out of Carrier Sense: Interference Cancellation for Wireless Lans," *Proc. ACM MOBICOM '08,* 2008.

[14] *IEEE Std. 802.15.4-2006: Wireless Medium Access Control and Physical Layer Specifications for Low-Rate Wireless Personal Area Networks,* IEEE Std., http://www.ieee802.org, 2003.

[15] S.P. Weber, J.G. Andrews, X.Y. Yang, and G. de Veciana, "Transmission Capacity of Wireless Ad Hoc Networks with Successive Interference Cancellation," *IEEE Trans. Information Theory,* vol. 53, no. 8, pp. 2799-2814, Aug. 2007.

[16] Y. Li, L. Guo, and S.K. Prasad, "An Energy-Efficient Distributed Algorithm for Minimum-Latency Aggregation Scheduling in Wireless Sensor Networks," *Proc. IEEE 30th Int'l Conf. Distributed Computing Systems (ICDCS '10),* 2010.

[17] X. Xu, X.-Y. Li, X. Mao, S. Tang, and S. Wang, "A Delay-Efficient Algorithm for Data Aggregation in Multihop Wireless Sensor Networks," *IEEE Trans. Parallel and Distributed Systems*, vol. 22, no. 1, pp. 163-175, Jan. 2011.
[18] B. Yu, J. Li, and Y. Li, "Distributed Data Aggregation Scheduling in Wireless Sensor Networks," *Proc. IEEE INFOCOM '09*, 2009.
[19] B. Yu and J. Li, "Minimum-Time Aggregation Scheduling in Multi-Sink Sensor Networks," *Proc. IEEE Eighth Ann. Comm. Soc. Conf. Sensor, Mesh, and Ad Hoc Com. and Networks (SECON '11)*, 2011.
[20] P. Balister, B. Bollobas, A. Anandkumar, and A. Willsky, "Energy-Latency Tradeoff for In-Network Function Computation in Random Networks," *Proc. IEEE INFOCOM '11*, 2011.
[21] O. Simeone, O. Somekh, Y. Bar-Ness, H.V. Poor, and S. Shamai, "Capacity of Linear Two-Hop Mesh Networks with Rate Splitting Decode-And-Forward Relaying and Cooperation," *Proc. IEEE 45th Ann. Allerton Conf. Comm., Control and Computing (Allerton '07)*, 2007.
[22] X. Wang and J. Garcia-Luna-Aceves, "Embracing Interference in Ad Hoc Networks Using Joint Routing and Scheduling with Multiple Packet Reception," *Proc. IEEE INFOCOM '08*, 2008.
[23] S. Lv, W. Zhuang, X. Wang, and X. Zhou, "Scheduling in Wireless Ad Hoc Networks with Successive Interference Cancellation," *Proc. IEEE INFOCOM '11*, 2011.
[24] C. Jiang, Y. Shi, Y.T. Hou, W. Lou, S. Kompella, and S.F. Midkiff, "Squeezing the Most Out of Interference: An Optimization Framework for Joint Interference Exploitation and Avoidance," *Proc. IEEE INFOCOM '12*, 2012.
[25] O. Goussevskaia and R. Wattenhofer, "Scheduling Wireless Links with Successive Interference Cancellation," *Proc. IEEE 21st Int'l Conf. Computer Comm. and Networks (ICCCN '12)*, 2012.
[26] P.J. Wan, K.M. Alzoubi, and O. Frieder, "Distributed Construction of Connected Dominating Set in Wireless Ad Hoc Networks," *Proc. IEEE INFOCOM '02*, 2002.
[27] L. Fu, S.C. Liew, and J. Huang, "Effective Carrier Sensing in CSMA Networks under Cumulative Interference," *Proc. IEEE INFOCOM '10*, 2010.
[28] *Sinaglo: Simulator for Network Algorithms*, http://www.disco.ethz.ch/projects/sinalgo/, 2013.
[29] H. Li, C. Wu, D.X. Yu, Q.S. Hua, and F.C.M. Lau, "Aggregation Latency-Energy Tradeoff in Wireless Sensor Networks with Successive Interference Cancellation," technical report, https://sites.google.com/site/hongxingli82/home/SIC.pdf, 2012.
[30] E.F. Beckenbach and R. Bellman, *Inequalities*. Springer-Verlag, 1965.
[31] H. Groemer, "Über Die Einlagerung Von Kreisen in Einen Konvexen Bereich," *Math. Z.*, vol. 73, pp. 285-294, 1960.
[32] C. Ambuhl, "An Optimal Bound for the MST Algorithm to Compute Energy Efficient Broadcast Trees in Wireless Networks," *Proc. 32nd Int'l Colloquium Automata Languages and Programming (ICALP '05)*, 2005.

Hongxing Li received the BSc and MEng degrees in 2005 and 2008 from the Department of Computer Science and Technology, Nanjing University, China, and the PhD degree in 2012 from the Department of Computer Science, The University of Hong Kong, Hong Kong. His research interests include wireless networks and cloud computing. He is a member of the IEEE.

Chuan Wu received the BEng and MEng degrees in 2000 and 2002, respectively, from the Department of Computer Science and Technology, Tsinghua University, China, and the PhD degree in 2008 from the Department of Electrical and Computer Engineering, University of Toronto, Canada. She is currently an assistant professor in the Department of Computer Science, the University of Hong Kong, Hong Kong. Her research interests include measurement, modeling, and optimization of large-scale peer-to-peer systems and online/mobile social networks. She is a member of the IEEE and ACM.

Dongxiao Yu received the BSc degree from the School of Mathematics, Shandong University, and is currently working toward the PhD degree in the Department of Computer Science, the University of Hong Kong. His research interests include wireless networks, distributed computing, and graph theory.

Qiang-Sheng Hua received the BEng and MEng degrees in 2001 and 2004, respectively, from the School of Information Science and Engineering, Central South University, China, and the PhD degree in 2009 from the Department of Computer Science, The University of Hong Kong, China. He is currently an assistant professor in the Institute for Interdisciplinary Information Sciences, Tsinghua University, China. His research interests include wireless networking and algorithms. He is a member of the IEEE and the IEEE Computer Society.

Francis C.M. Lau received the PhD degree in computer science from the University of Waterloo. He is currently a professor in computer science at The University of Hong Kong. He is the editor-in-chief of the *Journal of Interconnection Networks*. His research interests include computer systems, networks, programming languages, and application of computing in arts. He is a senior member of the IEEE and the IEEE Computer Society.